

# MIXED MODE DOUBLE CANTILEVER BEAMS TEST SPECIMEN FOR CHARACTERIZATION OF STRUCTURAL ADHESIVE JOINTS

J.C. Suárez<sup>1</sup>, P. Pinilla<sup>1</sup>, F. López<sup>1</sup>, M.A. Herreros<sup>1</sup>, M.V. Biezma<sup>2</sup>

<sup>1</sup>Research Group on Hybrid Materials, ETS Ingenieros Navales, Universidad Politécnica de Madrid, Avda. Arco de la Victoria, s/n, 28040 Madrid, Spain.  
E-mail: juancarlos.suarez@upm.es

<sup>2</sup>Departamento de Ciencia e Ingeniería del Terreno y los Materiales, Universidad de Cantabria, Dique de Gamazo s/n, 39004 Santander, Spain.  
E-mail: maria.biezma@unican.es

## ABSTRACT

Numerical simulations or virtual testing are gradually replacing many expensive and time consuming experiments in the product design process. To be able to predict the performance of the adhesive joints accurately, correct material data of adhesives are essential. Hence, it is critical to develop reliable testing methods to obtain the constitutive behaviour of adhesive layers. For adhesive joints, it is convenient to let the constitutive relation represent the mechanical behaviour of the entire adhesive layer. Such a constitutive relation describes activities in the adhesive layer before and at fracture. The objective of this work is to experimentally obtain the constitutive behaviour of an adhesive layer under mixed mode loading. The Mixed Mode Double Cantilever Beams (MCB) specimen used in the experiments is designed to allow the adhesive layer to be loaded by a force varying smoothly from pure peel to pure shear. An explicit J-integral expression is derived for the MCB-specimen and used to evaluate the energy dissipation in the FPZ. The measured deformations of the adhesive layer in the FPZ show a nonlinear deformation path in all tested mode mixities and the critical deformation of the adhesive in the peel direction is virtually independent of the mode mixity. The constitutive behaviour of the adhesive layer is obtained by the inverse method. The obtained constitutive behaviour of the mixed mode loaded adhesive layer is coupled and mode dependent.

**KEY WORDS:** adhesive, mixed mode, J-integral, virtual testing.

## 1. INTRODUCTION

Adhesive joints are designed in such a way that a thin layer of adhesive is placed between two substrates, which are usually stiffer than the polymeric adhesive system, thus constraining its displacements under load. There is experimental evidence that a thin layer of adhesive behaves differently compared to the bulk material [1].

Table 1. Decomposition methods by various researchers

	Descomposition method by
Reeder and Crews [3]	Load
Ducept et al. [4]	Load
Hutchinson and Suo [5]	SIF
Shapery and Davidson [6]	SIF
Thouless et al. [7]	ERR
Fernlund and Spelt [2]	ERR
Pang [8]	SIF

SIF: Stress Intensity Factor; ERR: Energy Release Rate

Adhesive joints are much stronger when loaded in shear than in peel. Much more difficult is to assess the properties in mixed mode loading I+II [2]. The approaches for analyzing mode mixities on adhesive

joints can be classified in two categories: the global approaches and the local approaches, as summarized in Table 1. The decomposition methods that are based on the input parameters are referred to as global approaches. The methods that are based on the output parameters in terms of the SIF and the ERR are referred to as local approaches

Among the *global approaches*, the Tapered Double Cantilever Beam (TDCB) specimen has been used by the authors and results presented elsewhere for pure mode I loading [9]. The mixed mode bending (MMB) specimen is very useful for achieving a range of mode mixities on an adhesive joint, as reported by the authors for elastic adhesives [10].

The *local approaches* focus on the local condition at the crack tip region of an adhesive joint, i.e., the ends of the overlap area, in terms of the SIF and the ERR. Under this category, three types of joint models are considered:

- Bi-material models, in which unbalances of the adherends are considered and the adhesive layer is ignored;
- Adhesive-layer models, in which the adhesive layer is modeled by, e.g., the embedded process zone (EPZ) model;

- Calibrated joint models, in which an adhesive joint is modeled and compared to a specimen without the adhesive layer by the use of a calibration factor.

The mode mixity can be achieved by introducing geometrical or material unbalances into a load-balanced joint, such as the Double Cantilever Beam (DCB) and Crack Lap Shear (CLS) specimen. However, neither the DCB nor the CLS can achieve mode mixity in the complete spectrum, i.e., from pure mode I to pure mode II. In general, to make valuable conclusions for experiments, a number of specimens are required for achieving the repeatability and the reliability. It is then more suitable to use one and the same geometry of the specimen and vary the loading system in order to achieve a range of mode mixities. In such a way, only one type of specimen has to be designed and manufactured. This sets design requirements on the loading system:

- *Flexibility*: the loading system should be simply adjustable for testing different mode mixities;
- *Variety*: the ability for attaining the entire spectrum of mode mixities, i.e., from pure mode I to pure mode II;
- *Stability*: the mode mixity should vary steadily and smoothly by a pre-defined adjusting parameter in the loading system.

Based on the geometry of a semi-infinite symmetric DCB-specimen, by combining the basic loading cases of DCB, ELS and CLS, a testing specimen, referred to as the mixed mode double cantilever beam (MCB) specimen, is suggested [11, 12].

## 2. MIXED MODE DOUBLE CANTILEVER BEAM (MCB) SPECIMEN

To experimentally obtain the constitutive behaviour of an adhesive layer, it is advantageous to restrict the number of process zones to one in the tested adhesive layer. This can be achieved by loading the specimen at one end and using a long specimen. Due to the elastic properties of the adhesive layer, the far end of the specimen will be virtually unloaded. Thus, a reasonably long specimen can be considered semi-infinite in the analysis. Figure 1 illustrates the mixed mode double cantilever beam (MCB) specimen as superposition of the basic loading systems. Each adherend at the free end of the MCB-specimen is loaded with an external force,  $F$ , with the same magnitude but opposite direction. This pair of forces are self-balancing and their direction of action is defined by the angle  $\alpha$ .

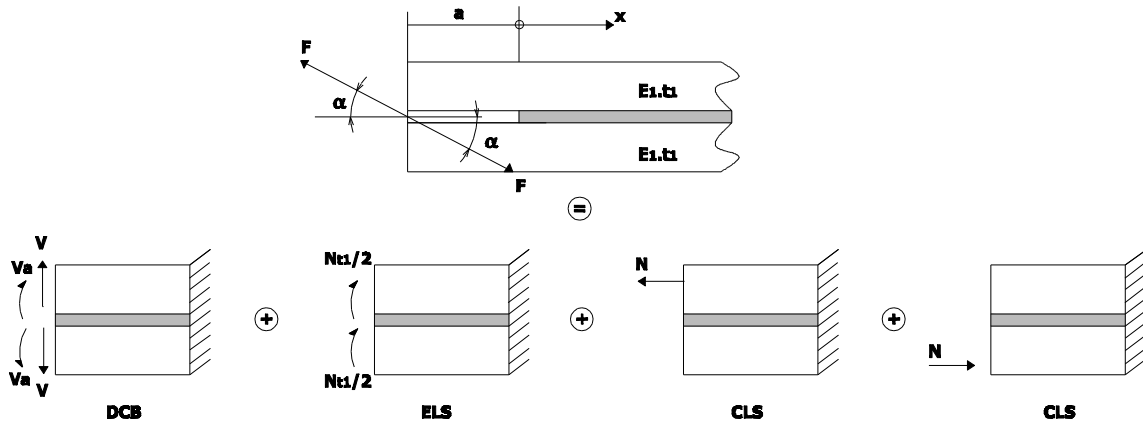


Figure 1. Mixed mode double cantilever beam (MCB) specimen as superposition of the basic loading systems.

The sectional forces at the crack tip,  $x = 0$ , in Figure 1 are

$$N = F \cos \alpha \quad (1)$$

$$V = F \sin \alpha \quad (2)$$

Superposition of the deformations for the basic loading systems gives the normal and tangential deformation at the crack tip

$$\hat{w} = \Delta \sin \beta = \frac{2\kappa_{pt}}{bE} (1 + \kappa_p a) F \sin \alpha \quad (3)$$

$$\hat{v} = \Delta \cos \beta = \frac{\kappa_s t}{bE} F \cos \alpha \quad (4)$$

where  $\Delta$  is the total deformation of the adhesive layer at the crack tip and  $\beta = \tan^{-1} \hat{w}/\hat{v}$  is the angle between the deformation modes. For a linear elastic MCB-specimen, the ERR is decomposed in mode I and mode II as

$$J_I = \frac{1}{2} \frac{\bar{E}}{t} \Delta^2 \sin^2 \beta = \frac{12}{E_1 t_1} \left( \frac{F}{b} \right)^2 \left( \frac{1}{\kappa_p t_1} + \frac{a}{t_1} \right)^2 \sin^2 \alpha \quad (5)$$

$$J_{II} = \frac{1}{2} \frac{G}{t} \Delta^2 \cos^2 \beta = \frac{4}{E_1 t_1} \left( \frac{F}{b} \right)^2 \cos^2 \alpha \quad (6)$$

With the mode mixity defined by

$$\Lambda = \frac{J_{II}}{J_I + J_{II}} \quad (7)$$

A combination of Eqs. 5, 6 and 7, gives the mode mixity of the MCB-specimen in terms of the force angle  $\alpha$

$$\Lambda \alpha = \frac{\cos^2 \alpha}{3 \left( \frac{1}{\kappa_p t_1} + \frac{a}{t_1} \right)^2 \sin^2 \alpha + \cos^2 \alpha} \quad (8)$$

In terms of the deformation angle  $\beta$

$$\Lambda \beta = \frac{\cos^2 \beta}{\frac{\bar{E}}{G} \sin^2 \beta + \cos^2 \beta} \quad (9)$$

### 3. EXPERIMENTAL PROCEDURE

The specimens are fabricated by first bonding two steel plates with 1 mm thick adhesive, then cut into desired width after curing. The plates are made of naval steel grade A, 10 mm in thickness, with material data given in Table 2. The adhesive is a two-components polyurethane system. To enhance the bonding surfaces, the plates are cleaned with acetone and sand grinded. Teflon film stripes of 0.5 mm are inserted between the plates to ensure an even thickness of the adhesive layer, as well as the crack tip position. After curing at 25 °C for 24 h, the joined plates are then cut into 4 mm wide specimens.

Table 2. Material and geometrical data for the MCB-specimen used in experiments

Overall joint	Bonded length, L=100 mm
	Joint width, b=4 mm
	Crack length, a=0 mm
Adherends	Naval steel plates, grade A
	Thickness, t <sub>1</sub> =10 mm
	Young modulus, E=207 GPa
	Yield strength, σ <sub>y</sub> =275 MPa
Adhesive	Two-components polyurethane
	Thickness, t=0.5 mm

Two fixture parts, Figure 2, are designed to allow the specimen to be loaded in an uniaxial tensile test machine. Seven different mode mixities can be achieved, with loading angles  $\alpha = 0^\circ, 15^\circ, 30^\circ, 45^\circ, 60^\circ, 75^\circ$  and  $90^\circ$ . Two forks are also manufactured to allow

the tensile machine to grip the fixtures at different angles. A electromechanic testing system, with loading capacity of  $\pm 5$  kN is used. The experiments are made at a constant displacement rate of 15  $\mu\text{m/s}$ . The loading force is recorded on a computer during the experiments.



Figure 2. Fixtures with the MCB-specimen.

Another set of test specimens has been aged in sea water, and the joints have been tested after different times of immersion in order to assess the degradation of the strength along the time. The results will be presented elsewhere.

### 4. RESULTS AND DISCUSSION

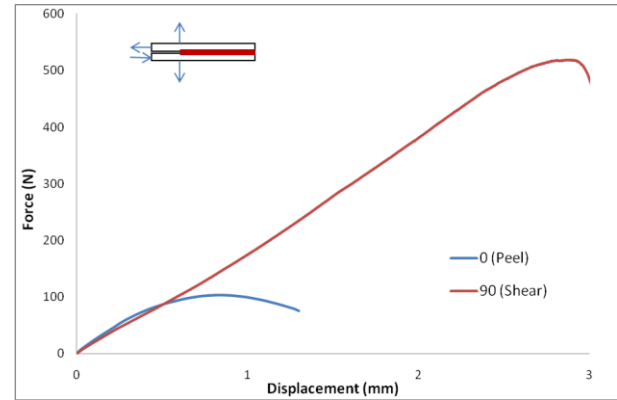


Figure 3. Loading histories for different mode mixities.

Evaluation of the energy dissipation and the constitutive relation of the adhesive layer is based on the J-integral. The parameters measured during the experiment are: the external force F, the rotation of the adherends  $w'_1$  and  $w'_2$  at the crack tip ( $x = 0$ ), and the deformation of the adhesive layer  $w$  and  $v$  at the crack tip ( $x = 0$ ). A total of 21 specimens are tested, with three specimens tested at each of the seven loading angles.

The loading histories for every mode mixities are shown in Figure 3 where the external force,  $F$ , is plotted against the total deformation of the adhesive layer at the crack tip,  $\Delta = \sqrt{w^2 + v^2}$ . No instability is observed;  $F$  increases to a maximum and then declines somewhat. One typical specimen is chosen from each loading angle, with increasing in shear loading from the bottom to the top.

The adherends remain elastic under the loading. For small deformation of the adherends, the rotations of the adherends at the crack tip are evaluated by

$$w'_1 = \frac{u_{x,1} - u_{x,2}}{y_1 - y_2} \quad w'_2 = \frac{u_{x,3} - u_{x,4}}{y_3 - y_4} \quad (10)$$

where  $u_{x,i}$  is the displacement in  $x$ -direction and  $y_i$  is the coordinate in  $y$ -direction of point  $i$ , where  $i = 1, 2, 3, 4$  (see Figure 4)

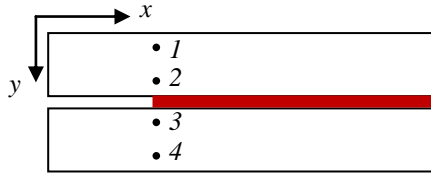


Figure 4. Displacement data of the four points and rotations of the adherends.

The rigid body rotation is given by

$$\gamma = \frac{w'_1 + w'_2}{2} \quad (11)$$

Thus, the true loading angle,  $\alpha$ , is the design loading angle,  $\alpha_{\text{design}}$ , modified by the rigid body rotation:  $\alpha = \alpha_{\text{design}} + \gamma$ .

The shear and peel deformation of the adhesive layer are defined as the differences of the longitudinal and vertical displacements of the adhesive/adherend interfaces relative to the orientation of the adhesive layer. To define these, the deformations relative to the fixed coordinate system are first given

$$v_o = u_{x,3} - u_{x,2} \quad w_o = u_{y,3} - u_{y,2} \quad (12)$$

With consideration to the rigid body rotation  $\gamma$ , the deformations become

$$v = v_o + w_o \tan \gamma \quad w = w_o - v_o \gamma \quad (13)$$

where  $t$  is the thickness of the adhesive layer.

The chosen MCB-specimen geometry has a crack length  $a = 0$  and the expression for the J-integral is [12]

$$J = \frac{F \sin \alpha}{b} (w'_1 - w'_2) + \frac{4}{E t_1} \left( \frac{F \cos \alpha}{b} \right)^2 \quad \dots\dots (14)$$

The variables  $F$ ,  $w'_1$  and  $w'_2$  in Eq. (14) are measurable in an experiment, which enables the evaluation of the constitutive behaviour of the adhesive layer in terms of stress-deformation relationships, as obtained by partial differentiation

$$\sigma_{w,v} = \frac{\partial J_{adh}}{\partial w} \quad \tau_{w,v} = \frac{\partial J_{adh}}{\partial v} \quad (15)$$

This approach implicitly assumes that the cohesive stresses are derived from a potential function, i.e. that  $J_{adh}$  does not depend on the deformation path, just on  $w$  and  $v$ . This method is referred to as the inverse method to determine the constitutive behaviour of a material through the overall response of the structure.

The MCB-specimen with  $a=0$  satisfies all the requirements set on the loading system. That is the entire spectrum of mode mixity can be achieved smoothly by one pre-defined adjusting parameter: the loading angle  $\alpha$ . However, the theory for obtaining the constitutive behaviour of the adhesive layer sets more requirements on the MCB-geometry:

1. In order to be able to treat the adhesive layer as a continuous distribution of bi-directional springs, the adhesive layer should be thin and flexible in comparison with the adherends. This requirement sets a condition on the relative stiffness of the adherends as compared to the adhesive as
- $$\frac{E_1 t}{E t_1} > 0.1 \quad (16)$$
2. The model is based on small deformations. Thus, a requirement is that the deformation of the adhesive layer at the crack tip is small in comparison with the overall dimensions of the joint.
  3. The overlap length should be long since the specimen is considered as semi-infinite in the derivation of equations.
  4. The adherends should deform linear elastically. Thus, the maximum stress in the adherends at  $x=0$  should be smaller than the yield strength of the adherends.
  5. It should be possible to exceed the fracture energy in all mode mixities. The fracture energy in mode II,  $J_{IIc}$ , is much larger than the fracture energy in mode I,  $J_{Ic}$ . It is then assumed that the maximum fracture energy is attained in pure mode II.

The adherends are modeled as Euler–Bernoulli beams and the adhesive layer is modeled by interphase elements. The cohesive behaviour of the adhesive layer is modeled by the normalised cohesive law, which is governed by the cohesive behaviour of the adhesive layer in pure mode I and mode II. The experiments are simulated with the commercial FE-program ABAQUS (v6.4), see Figure 5. The inverse method is then used to

extract the constitutive behaviour of the adhesive layer under mixed mode loading.

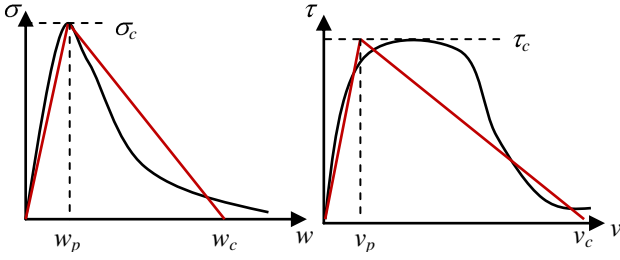


Figure 5. The saw-tooth model simplifies the cohesive behaviour of the adhesive layer.

The cohesive behaviour of the adhesive layer, or stress–deformation relations, are conveniently simplified by a saw-tooth shaped curve. Although differing from the real constitutive behaviour, the saw-tooth model capture the characteristic cohesive parameters of the adhesive layer.

A dimensionless deformation measure  $\lambda$  is defined by

$$\lambda^2 = \bar{v}^2 + \bar{w}^2 = \left( \frac{v}{v_c} \right)^2 + \left( \frac{w}{w_c} \right)^2 \quad (17)$$

where  $\bar{w}$  and  $\bar{v}$  are the normalised normal and tangential deformation, respectively. Softening behaviour of the adhesive layer begins when  $\lambda = \lambda_p$ , which is given by

$$\lambda_p^2 = \frac{\bar{v}_p^2 \bar{w}_p^2}{\bar{v}_p^2 \sin^2 \theta + \bar{w}_p^2 \cos^2 \theta} \quad (18)$$

where  $\theta = \tan^{-1} \bar{w}/\bar{v}$ . For each value of  $\theta$ , the normalised stress,  $S$ , is defined by

$$S_{\lambda, \theta} = \begin{cases} \frac{\lambda}{\lambda_p \theta} & \text{when } 0 < \lambda < \lambda_p \\ \frac{1-\lambda}{1-\lambda_p \theta} & \text{when } \lambda_p < \lambda < 1 \\ 0 & \text{when } \lambda > 1 \end{cases} \quad (19)$$

According to Eq. (19), Figure 6 shows the graphical presentation of the mixed mode cohesive law in the dimensionless form

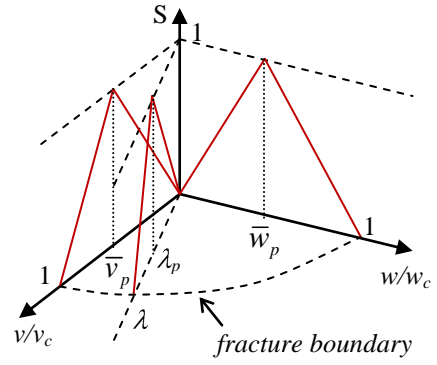


Figure 6. Graphical presentation of the mixed mode cohesive law.

## 5. CONCLUSIONS

1. Different mixed mode loaded specimen configurations are investigated. The decomposition methods of mode mixity in a joint can be classified into the global approaches and the local approaches. The mode mixity of an adhesive layer is due to unbalances in the loading system and/or unbalanced in the material and/or geometrical properties of the adherends.
2. A specimen for testing adhesive layers under mixed mode loading, the mixed mode double cantilever beam (MCB) specimen, is proposed based on the basic loading systems. The dimensioned MCB-specimen satisfies all requirements set on the loading system as well as the evaluation criteria.
3. A mixed mode constitutive law of the adhesive layer can be determined by the use of the J-integral.
4. The FE-simulations can catch the overall shape of the mixed mode constitutive law. The inverse method is then used to extract the constitutive behaviour of the adhesive layer under mixed mode loading.

## ACKNOWLEDGEMENTS

The authors acknowledge the support from Universidad Politécnica de Madrid through grant AM0402. Our gratitude to the laboratory technical staff: Mr. José Illescas, Ms. Ana Soria, and Ms. Ana García for their assistance in the completion of these experiments.

## REFERENCES

- [1] Jeandrau, JP, Int J Adhesion and Adhesives, pag. 11-71, 1991.

- [2] Fernlund G, Spelt JK. Mixed mode energy release rate for adhesively bonded beam specimen. *J Compos Technol Res* 16(3), pag. 234–243, 1994.
- [3] Reeder JR, Crews JH. Mixed-mode bending method for delamination testing. *AIAA J* 28(7), pag. 1270–1276, 1990.
- [4] Ducept F, Gamby D, Davies R. A mixed-mode failure criterion derived from tests on symmetric and asymmetric specimens. *Compos Sci Technol*, 59, pag. 609–619, 1999.
- [5] Hutchinson JW, Suo Z. Mixed mode cracking in layered materials. *Adv Appl Mech*, 29, pag. 63–191, 1992.
- [6] Shapery RA, Davidson BD. Prediction of energy release rate for mixed-mode delamination using classical plate theory. *Appl Mech Rev*, 43(5), pag. 281–287, 1990.
- [7] Li S, Thouless MD, Waas AM, Schroeder JA, Zavattieri PD. Mixed-mode cohesive-zone models for fracture of an adhesively bonded polymer–matrix composite. *Engng Fract Mech*, 73, pag. 64–78, 2006.
- [8] Pang HLJ, Seetoh CW. A compact mixed mode (CMM) fracture specimen for adhesive bonded joints. *Engng Fract Mech*, 57(1), pag. 57–65, 1997.
- [9] Suarez JC, Herreros MA, Pinilla P, Miguel S, López F. Energía de fractura en uniones adhesivas de materiales híbridos fibra-metal: ensayos TDCB modificados. *Anales de la Mecánica de la Fractura*, vol. 1, pag. 229–234, 2007.
- [10] Suárez JC, López F, Miguel S, Pinilla P, Herreros MA. Determination of the mixed-mode fracture energy of elastomeric structural adhesives: evaluation of debonding buckling in fibre–metal hybrid laminates. *Fatigue & Fracture Eng. Mat & Struct*, 32 (2), pag. 127–140, 2009.
- [11] Högberg JL, Stigh U. Specimen proposals for mixed mode testing of adhesive layer. *Engng Fract Mech*, 73, pag. 2541–2556, 2006.
- [12] Högberg JL, Sørensen BF, Stigh U. Constitutive behaviour of mixed mode loaded adhesive layer. *International Journal of Solids and Structures* 44 8335–8354, 2007.